Setd1a Plays Pivotal Roles for the Survival and Proliferation of Retinal Progenitors via Histone Modifications of Uhrf1

Xiaoyue Deng,[1] Toshiro Iwagawa,[1] Masaya Fukushima,[1,2] Yutaka Suzuki,[3] and Sumiko Watanabe[1]

[1]Division of Molecular and Developmental Biology, Institute of Medical Science, The University of Tokyo, Tokyo, Japan
[2]Department of Ophthalmology, The University of Tokyo, Tokyo, Japan
[3]Department of Medical Genome Sciences, Graduate School of Frontier Sciences, The University of Tokyo, Chiba, Japan

Correspondence: Sumiko Watanabe, Division of Molecular and Developmental Biology, Institute of Medical Science, The University of Tokyo, 4-6-1 Shirokane-dai, Minato-ku, Tokyo 108-8639, Japan; sumiko@ims.u-tokyo.ac.jp.

Received: January 6, 2021
Accepted: April 2, 2021
Published: May 3, 2021

Citation: Deng X, Iwagawa T, Fukushima M, Suzuki Y, Watanabe S. Setd1a plays pivotal roles for the survival and proliferation of retinal progenitors via histone modifications of Uhrf1. *Invest Ophthalmol Vis Sci.* 2021;62(6):1. https://doi.org/10.1167/iovs.62.6.1

Purpose. The trimethylation of histone H3 at lysine 4 (H3K4me3) facilitates transcriptional gene activation, and *Setd1a* is the methyltransferase specific to H3K4. H3K4me3 has been reported to regulate rod photoreceptor differentiation; however, the roles H3K4me3 plays in retinal progenitor cell (RPC) proliferation and differentiation during early retinal development remain unclear.

Methods. Using an in vitro retinal explant culture system, we suppressed the expression of *Setd1a* by introducing shSetd1a. We examined the expression level and H3K4me3 level of genes by RNA Sequencing and ChIP assay, respectively.

Results. We found that *Setd1a* depletion resulted in increased apoptosis and proliferation failure in late RPCs. Expression of wild-type SETD1A, but not SETD1A that lacked the catalytic SET domain, reversed the shSetd1a-induced phenotype. RNA Sequencing revealed that proliferation-related genes were downregulated upon shSetd1a expression. Based on publicly available H3K4me3-ChIP sequencing data of retinal development, we identified *Uhrf1* as a candidate target gene of *Setd1a*. The expression of shSetd1a led to a decrease in *Uhrf1* transcript levels and reduced H3K4me3 levels at the *Uhrf1* locus. Increased apoptosis and the suppression of proliferation in late RPCs were observed in retinal explants expressing shUhrf1, similar to the outcomes observed in shSetd1a-expressing retinas. The overexpression of UHRF1 did not rescue shSetd1a-induced apoptosis, but reversed the suppression of proliferation.

Conclusions. These results indicate that *Setd1a* contributes to the survival and proliferation of retinal cells by regulating histone methylation, *Setd1a* regulates *Uhrf1* expression, and these two molecules cooperate to regulate RPC survival and proliferation.

Keywords: histone methylation, RNA seq, H3K4, mouse, explant

The retina is part of the central nervous system, and retinal explant culture is an excellent model for analyzing molecular mechanisms underlying developmental processes. During retinal development, retinal progenitor cells (RPCs) proliferate and differentiate into six types of neurons and one type of glial cell. The temporal order by which each type of retinal cell is produced is highly regulated and conserved among species.[1] The molecular mechanisms by which cell fate is determined and maturation is accomplished have been investigated intensively, and much attention has been paid to the roles transcription factors play in retinal development.[2,3] Moreover, the contributions of epigenetic modifications, such as DNA methylation and histone modifications, to retinal development are becoming clearer.[4–6] We have been studying epigenetic histone modifications during retinal development and, with others, found that histone H3 methylation at lysine 4 (H3K4) and 27 was highly specific to retinal cell type. Additionally, analyses of knockout mice have revealed the functions of enzymes involved in these processes, especially H3 methylation at lysine 27 methylation.[7,8] At least nine histone lysine methyltransferases and five histone lysine demethylases have been reported to be involved in H3K4 methylation.[9] *Kdm5b*, a demethylation enzyme, participates in the determination of rod photoreceptor cell fate.[10] We found high levels of H3K4me3 in photoreceptor-related genes in rod photoreceptor lineage.[11] However, involvement of H3K4 methylation in early retinal development is not well-documented.

Setd1a (*Kmt2f*) encodes the member of a Set/COMPASS complex[12] and catalyzes H3K4me3.[13] *Setd1a* contains a SET [Su(var)3-9, Enhancer-of-zeste, Trithorax] domain at its C-terminus, which is a catalytic domain responsible for H3K4 histone methyltransferase activity.[14,15] *Setd1a* is required for embryonic, epiblastic, and neural stem cell survival, and gene knockout of *Setd1a* in mice led to rapid losses of bulk H3K4 methylation and a severe decrease in cell proliferation during embryonic development.[16] *Setd1a* also helps to maintain genome stability under replication stress through its

methylation function.[17,18] In addition, *Setd1a* has nonenzymatic roles, such as regulating DNA damage-response genes via its FLOS domain.[19]

Setd1a is highly expressed in the murine brain, especially in the neocortex. *Setd1a* haploinsufficiency affects the development of cortical axons, dendrites, and spines, resulting in cognitive defects.[20–22] Mutations of *SETD1A* have been found in human neurodevelopmental disorders such as schizophrenia.[21]

In the retina, the roles *Setd1a* plays in retinal development or diseases have not been documented. In this study, we examined the functions of *Setd1a* via short hairpin RNA (shRNA)-mediated the downregulation of *Setd1a* during retinal development. We found that *Setd1a* is essential for the survival and proliferation of late-stage RPCs. RNA sequencing (RNA-Seq) was performed to compare gene expression patterns between control and shSetd1a-expressing retinal cells, and *Uhrf1* was identified as a possible target. *Uhrf1* loss of function also resulted in apoptosis and proliferation failure. Interestingly, ectopic expression of UHRF1 reversed shSetd1a-induced suppression of proliferation but not the induction of apoptosis. Our results indicate that *Setd1a* and *Uhrf1* play critical roles during early retinal development.

Methods

Animals

All animal experiments were approved by the Animal Care Committee of the Institute of Medical Science, University of Tokyo, and conducted in accordance with the ARVO (Association for Research in Vision and Ophthalmology) statement for the use of animals in ophthalmic and vision research. Institute of Cancer Research (ICR) mice were obtained from Japan SLC Co.

RT-Quantitative PCR and shRNA Plasmids Construction

Total RNA was purified from the mouse retina using Sepasol RNA I Super G (Nacalai Tesque, Kyoto, Japan), and cDNA was synthesized using ReverTra Ace qPCR RT Master Mix (Toyobo, Osaka, Japan). Quantitative PCR (qPCR) was performed by the SYBR Green-based method with the Roche Light Cycler 96 (Roche Diagnostics). *Actb* and *Gapdh* were used as internal controls. Primer sequences are as follows: *Actb*_f:5′-ccaaccgcgagaagatga-3′, *Actb*_r: 5′-ccagaggcgtacagggatag-3′, *Gapdh*_f: 5′-tgaccacagtccatgccatc-3′, *Gapdh*_r: 5′-cataccaggaaatgagcttgac-3′, *Setd1a*_f: 5′-ggcaacatcattcatgccca-3′, *Setd1a*_r; 5′-gataggcagctgtgtccgag-3′, *Setd1b*_f: 5′-ggatgaaggcatcggtagca-3′, and *Setd1b*_r: 5′-gatcaccttggcgtagcagt-3′. Construction of the shRNA plasmids were done as described previously.[23] The target sequences (shSetd1a_1st: 5′-aaggatatgtgccggaaatatgg-3′, shSetd1a_2nd: 5′-aagctaaaccagctcaagtttcg-3′, shUhrf1_1st: 5′-aagaggctttccagtgcatctgc-3′, and shUhrf1_2nd: 5′-aagcggatgacaagactgtgtgg-3′, shSetd1b: 5′-aagttacaagttgatgattgacc-3′) were determined by using siDirect (http:// sidirect2.rnai.jp). The first and second shRNAs for both *Setd1a* and *Uhrf1* showed essentially the same results in the critical experiment, and representative data obtained by shRNA_firsts are shown in the figures.

DNA Construction of Overexpression of *Setd1a* and *Uhrf1*

Full-length *Setd1a* cDNA was cloned by PrimeSTAR GXL DNA Polymerase (Takara, Maebashi, Japan) using cDNA from mouse retina. PCR product was subcloned into pGEM-T Easy vector (Promega, Madison, WI). shSetd1a-resisitant *Setd1a* contains substitutions of the third bases of four amino acid, which do not affect the encoded amino acids by inverse PCR using the KOD-Plus-Mutagenesis Kit (Toyobo). The resultant fragment was substituted with the corresponding region of wild-type *Setd1a* by *Xho*I and *Eco*RV sites. *Setd1a* mutant lacking SET domain (from AA 1577 to 1700) was constructed by KOD-Plus-Mutagenesis Kit (Toyobo). The full-length *Uhrf1_HA* was purchased from Sino Biological (MG53591-CY, China), and shUhrf1-resistant *Uhrf1* was made by inverse PCR using the KOD-Plus-Mutagenesis Kit (Toyobo). All the cDNAs for over-expression were subcloned into pCAG-KS.

Electroporation and Retinal Explant Culture

In vitro electroporation and retinal explant culture were performed as described previously.[24,25] To trace plasmid-transfected cells, we cotransfected an enhanced green fluorescent protein (EGFP)-expression plasmid (pCAG-EGFP) with shRNA expression plasmid. The total amount of plasmids used for electroporation was 100 µg for each retina and composition of plasmids is empty or shRNA (70 µg) and pCAG-EGFP (30 µg) or shRNA (40 µg), pCAG or pCAG-rescue cDNA (40 µg) and pCAG-EGFP (20 µg). In some cases, to avoid apoptosis, retinas were cultured for 3 days in the presence of the pan-Caspase inhibitor Z-VAD-FMK (AdooQ BioScience, A12373; Irvine, CA) at 20 µM in the final concentration. For all the samples, we performed at least three independent electroporation with the same condition and counted cells from two or three sections in each sample.

Immunohistochemistry

Immunostaining of frozen sections was done as described previously.[24,25] Primary antibodies used were mouse monoclonal antibodies against Ki67 (BD Bioscience, 550609; San Jose, CA), HuC/D (Molecular Probes, A-21271; Euegene, OR), TFAP2A (DSHB, 3B5; Iowa City, Oiwa), cyclin D3 (Santa Cruz Biotechnology, sc-182; Santa Cruz, CA), NR2E3 (photoreceptor-specific nuclear receptor) (PP-H7223-00, PPMX; R&D Systems, Minneapolis, MN), glutamine synthetase (MAB302; Chemicon, Tokyo, Japan), SETD1A (Abcam, ab70378; Camridge, UK), and 5-methylcytosine (5mC) (Active Motif, 39649; Carlsbad, CA), sheep polyclonal antibody against CHX10 (Exalha Biologicals, Shirley, MA), goat polyclonal antibody against BRN3B (Santa Cruz, sc-6026), chick polyclonal antibody against GFP (Clontech, Mountain View, CA), and rabbit polyclonal antibody against active Caspase 3 (Promega, G748A). To optimize the 5mC signal, careful titration of hydrochloric (HCl) acid treatment before blocking and labelling was performed. Briefly, after wash with PBS for 10 minutes, retinal sections were permeabilized with 0.1% Triton X-100 for 10 minutes at room temperature and denatured for 15 minutes with freshly made 2 N HCl at 37°C. Then, retinal sections were neutralized with 0.1 M Tris-HCl (pH 8.0) for 10 minutes at room temperature. Nuclei were counterstained with 4′,6-diamidino-2-phenylindole, dihydrochloride (DAPI). Sections were then

Investigative Ophthalmology & Visual Science

treated with Alexa-488- or Alexa-594- conjugated appropriate secondary antibodies. Photos were taken under observation using Zeiss (Jena, Germany) Axio Image M1 and Axio Image M2.

EdU Incorporation Assay

For pulse labeling with 5-ethynyl-2'-deoxyuridine (EdU) to detect S-phase cells was performed by using Click-iT Plus EdU Cell Proliferation Kit for Imaging (Thermo Fisher Scientific, C10639; Waltham, MA). EdU was present in retinal explant culture medium at 10 µM as final concentration for 15 hours before fixation. Then, frozen sections of the explant retina were made, and the sections were treated with 2% BSA/PBS for 1 hour followed by permeabilization with 0.5% Triton X-100 in PBS for 20 minutes at room temperature. Then, sections were incubated the reaction cocktail for 1 hour and nuclei were counterstained with Hoechst 33342. Photographs were taken under observation using Zeiss Axio Imager M1 and Axio Imager M2, and the calculation of EdU-positive cells was based on nuclear-positive staining.

Determination and Quantification of Immunolabeled Cells

To make frozen sections (14 µm thickness), retinal areas within a 250-µm radius from the center of retinal optic nerve head were chosen. After immunostaining of retinal sections with indicated antibodies, photo-images of the same antibody staining were taken with same setting (Zeiss AxioVison software). Labeled cells were determined and quantified manually by one person with consistent principles. Details are as follows. The total number of cells in a certain square content was determined by DAPI-stained signals with the same luminance of fluorescence, and the number of transfected cells was determined by DAPI and EGFP with a superimposed luminance of florescence. Antibodies anti-retinal subtype specific marker positive cells were determined by colabelling of DAPI and specific antibodies. Transfected cells expressed specific marker proteins were determined by DAPI, EGFP and specific staining with a superimposed luminance. Independent three sections of one condition were chosen to undergo cell quantification, and labeled cells at three independent areas of 100 µm vision in each section were quantified.

RNA-Seq

Retinas (E17) were electroporated with either control or shSetd1a plasmid and cultured for 2 days. EGFP positive cells (~3e4 cells for 1 sample) were collected by a cell sorter, FACS Aria II (BD Biosciences) as described.[26] Total RNA of three control and four shSetd1a samples was extracted using Sepasol RNA I Super G (Nacalai tesque) and quantified by using a 2100 Bioanalyzer (Agilent Technologies). Using 1 ng of total RNA, cDNA was prepared and amplified by PCR by SMART-Seq v4 Ultra Low Input RNA Kit for Sequencing (Takara) according to the manufacturer's instructions. The RNA-Seq libraries were prepared using the amplified cDNA and Nextera XT DNA Sample Preparation Kit (Illumina). 36 bp of single read sequencing was conducted by HiSeq3000 sequencer (Illumina). The GEO accession number of RNA-Seq data is GSE154498.

Data Analysis of RNA-Seq Results

Sequenced reads were mapped to the mouse transcriptome (GENCODE GRCm38.p6) with salmon v0.11.3.[27] Salmon output was converted using wasabi v0.3[27] and loaded into sleuth v0.30.0[28] for further downstream analysis including statistical testing and visualization. Gene ontology (GO) term enrichment analysis was performed using the Database for Annotations, Visualization and Integrated Discovery (DAVID) with "GO_BP" (gene ontology biological processes) terms.[29,30]

Chromatin Immunoprecipitation (ChIP)-qPCR Assay

ChIP-qPCR was done as previously described.[31] Antibodies used for ChIP assay were as follows: antihistone H3 tri-methyl Lys4 (H3K4me3) antibody (Active motif), and rabbit control IgG (Cell Signaling). Primer sequences are as follows; *Uhrf1*_A_F: 5'-aggtcaaagtttgtccagctca-3', *Uhrf1*_A_R 5'-gggagacttccaccccaatt-3', *Uhrf1*_B_F 5'-gctcacttgggtcttcagcc-3', *Uhrf1*_B_R 5'-ctctgcagatctcaccccac-3', *Uhrf1*_C_F 5'-gagattcaattgtcgcgccc-3', and *Uhrf1*_C_R 5'-aaactcacctgaaccccacc-3'.

Reanalysis of Public ChIP-seq Data

H3K4me3 ChIP-seq reads from P0 retina and the corresponding input reads from GSE87064[32] were aligned to GRCm38 by Bowtie2 2.4.1[33] with default parameters. The aligned data were converted to BAM files by SAMtools 1.10.[34,35] MACS2 2.2.71[36] was then used for peak calling with the cutoff of $q < 0.05$, and the peaks were annotated by ChIPseeker 1.5.1.[37]

Statistical Analysis

Statistical analysis was performed using R software (The R Foundation for Statistical Computing, Vienna, Austria). The p-values were calculated by Student *t*-test or Tukey's test as indicated in the figure legend.

Results

Changes in Setd1a Expression Levels During Retinal Development

The expression pattern of *Setd1a* transcripts during retinal development was examined via RT-qPCR using RNAs extracted from whole mouse retinas at different developmental stages (Fig. 1A, left panel). Previous RNA-Seq analysis of developing mouse retinas (GSE87064) confirmed that *Setd1a* expression levels gradually decreased during retinal development (Fig. 1A, right panel). *Setd1a* transcript levels were relatively high before a birth, then gradually decreased. Levels likely stayed low until week 8.

The spatial expression pattern of the SETD1A protein was then examined via immunohistochemistry using frozen retinal sections. SETD1A was expressed at high levels across the entire embryonic retina, and gradually disappeared from the neuroblast layer during the postnatal stages (Fig. 1B). Staining with Ki67 proliferation antigen revealed that SETD1A was expressed in both proliferating and post-mitotic cells. Furthermore, SETD1A was expressed in amacrine cells (HuC/D; Fig. 1C) and retinal ganglion cells (BRN3B; Fig. 1D)

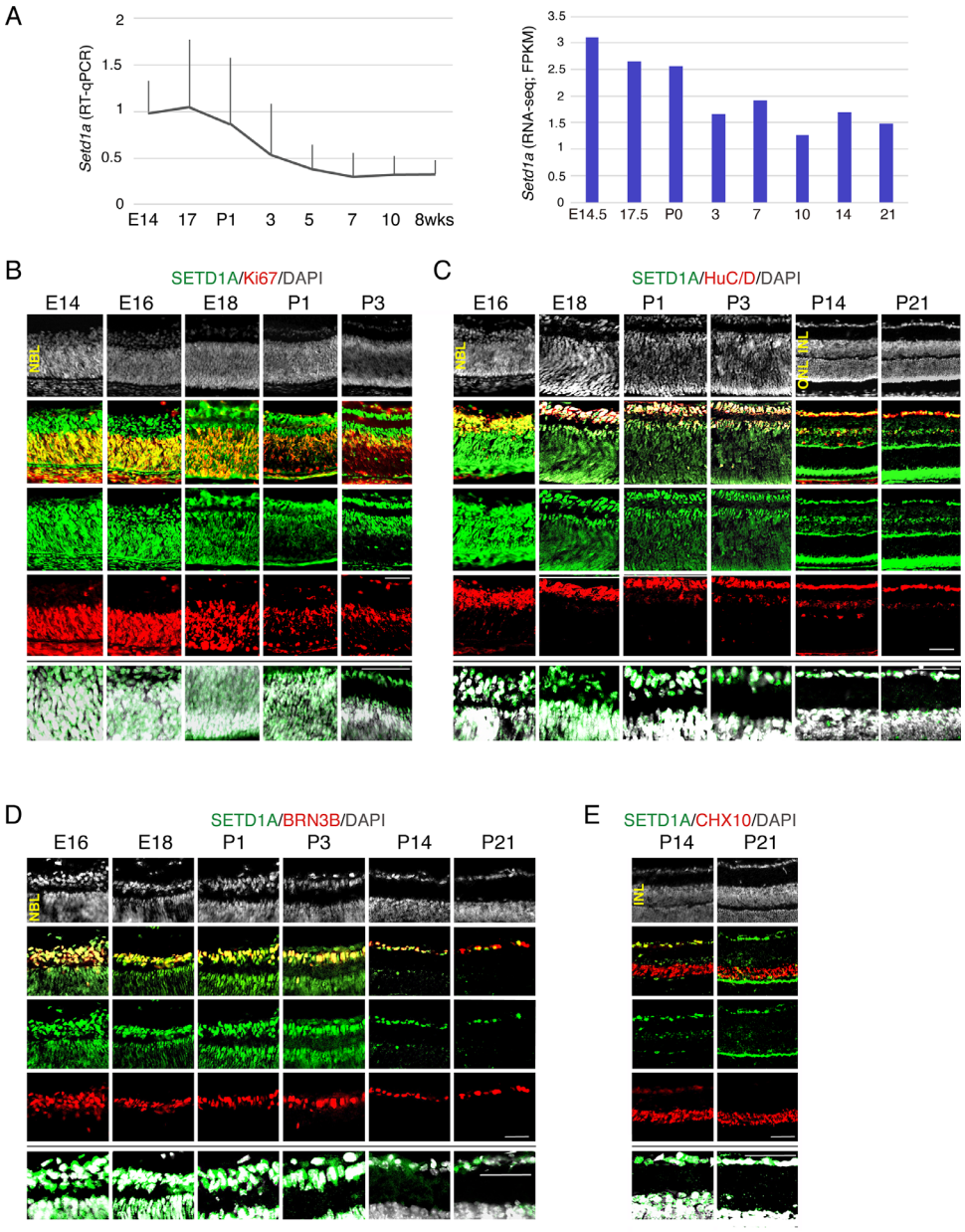

Figure 1. Transition of expression levels of Setd1a during retinal development. **(A)** Transition of expression level of transcripts of *Setd1a* during mouse retinal development was examined by RT-qPCR (*left*) and RNA-Seq analysis (*right*) of developing mouse retinas (GSE87064). (*Left*) Mouse whole retinas at indicated developmental stages were isolated, and RT-qPCR was performed. Relative expression levels of *Setd1a* to *Actb* and *Gapdh* are shown. The values are average of 3 independent samples with standard deviation. (*Right*) Fragments per kilobase of exon per million reads mapped (FPKM) value of RNA-Seq data. **(B–E)** Expression pattern of SETD1A protein in developing retinal cells was examined by immunohistochemistry. Mouse retinas at indicated developmental stages were frozen sectioned, and immunostaining by using indicated antibodies was performed. Nuclei were visualized by staining with DAPI. Bottom panels in B–E were enlarged staining patterns of SETD1A (*green*) and DAPI (*white*). Strong signals with anti-SETD1A antibody observed in the outer segment of P14 and P21 images were likely from nonspecific background staining. NBL, neuroblastic layer; INL, inner nuclear layer; ONL, outer nuclear layer. Scale bar = 50 µm.

but not in bipolar cells (CHX10; Fig. 1E). The SETD1A signals were overlapped with DAPI in the all stages, indicating the nuclear localization of SETD1A (Figs. 1B–E).

Downregulation of Setd1a Expression Led to Apoptosis and Suppressed RPC Proliferation in Developing Retinas

To elucidate the roles of *Setd1a* in retinal development, we examined the effects of shRNA-mediated downregulation of *Setd1a* during retinal development using retinal explant culture, which mimics retinal development in an *in vitro* tissue culture system. We electroporated plasmids encoding shSetd1a or control with EGFP-expressing plasmids into isolated mouse retinas on E17, and the retinas were cultured for 3 days as explants and then harvested. Significant reduction of the *Setd1a* expression in retinal explant was confirmed by RT-qPCR (Fig. 2A). The reduced level of SETD1A signal was also observed by immunohistochemistry (Fig. 2A). Apoptosis and proliferation were examined by staining cells with anti-active Caspase 3 (AC3) and anti-Ki67

Investigative Ophthalmology & Visual Science

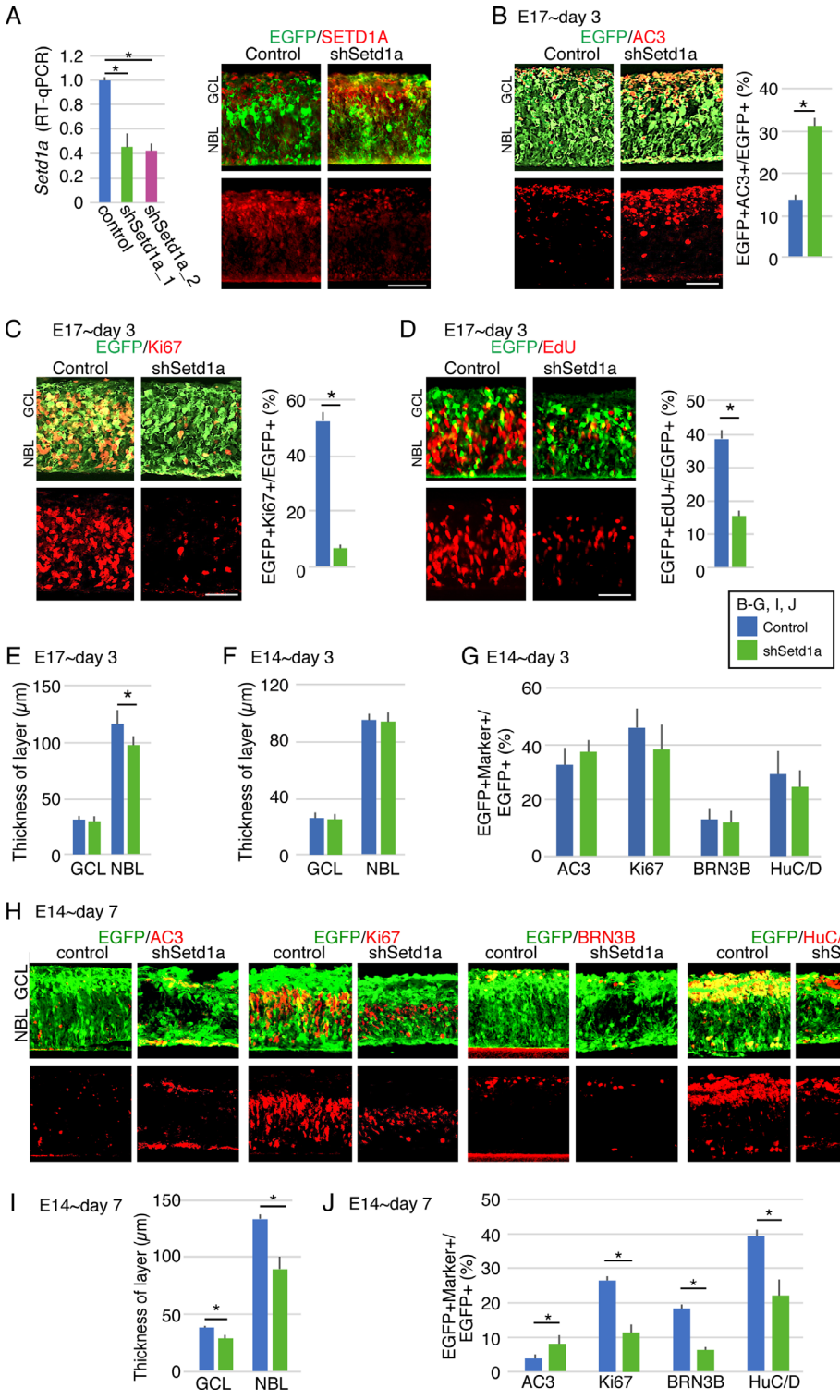

Figure 2. Downregulation of Setd1a expression increased apoptosis and decreased proliferation in the developing retina. Plasmids encoding control or shSetd1a, in combination with EGFP expression plasmids were electroporated into the retina derived from E17 **(A–E)** or E14 **(F–J)** embryos, and retinas were harvested after 3 days **(A–G)** or 7 days **(H–J)** of explant culture. After sorting EGFP-positive cells, RT-qPCR was performed, and the averages of 3 independent samples with standard deviations are shown in A. Immunohistochemistry was done by using anti-GFP, -active Caspase 3 (AC3) antibody to detect apoptotic cells **(B, H)** or anti-Ki67, proliferation antigen, antibody **(C, H)**. The incorporated EdU was detected by a click reaction **(D)**. Differentiation to retinal ganglion cells and amacrine cells were examined by staining with anti-BRN3B and -HuC/D antibodies, respectively **(H)**. Populations of AC3, Ki67, EdU, BRN3B, or HuC/D and EGFP double-positive cells in total EGFP-positive cells are shown in B, C, D, G, and J. Thickness of GCL and NBL were measured **(E, F, I)**. Values are average of at least three independent samples with standard deviation. *$p < 0.05$ (Student *t*-test). Scale bar = 50 μm. GCL, ganglion cell layer; NBL, neuroblastic layer.

Investigative Ophthalmology & Visual Science

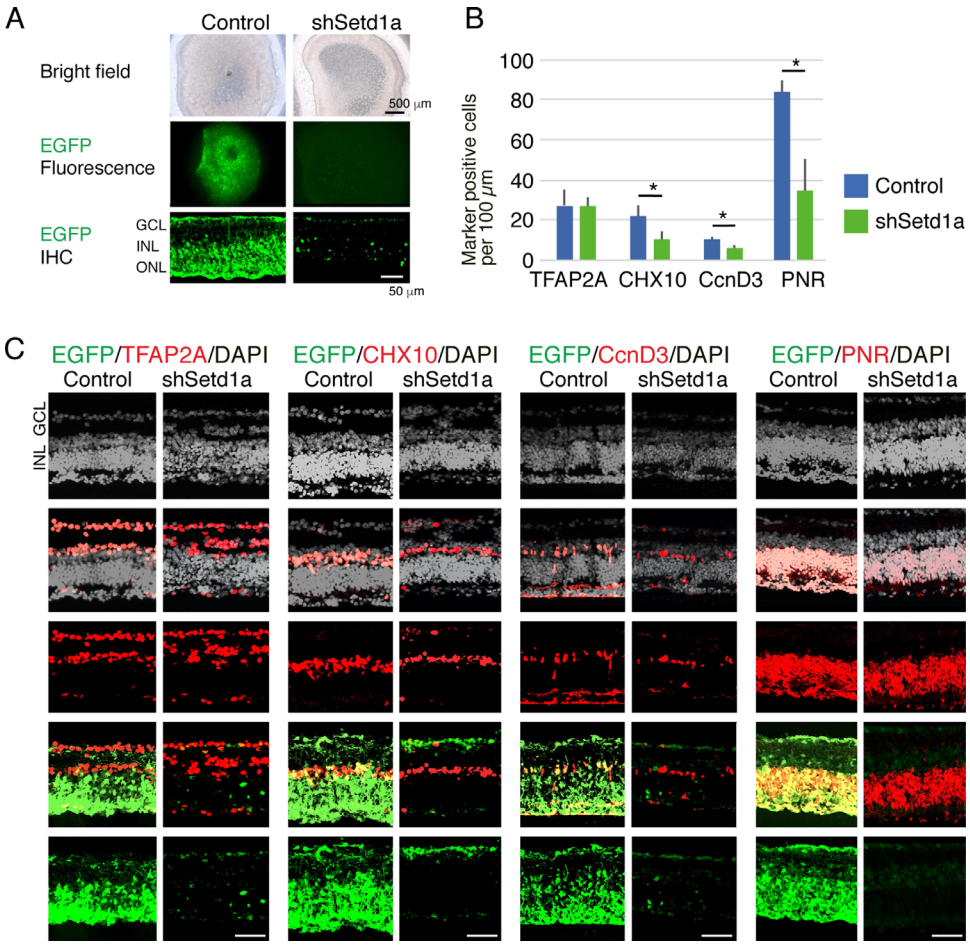

Figure 3. shRNA-mediated Setd1a depletion affected differentiation of late-born retinal subtypes. Retinas from E17 embryos were transfected with control- or shSetd1a- together with EGFP-expression plasmids and cultured as explants for 14 days. **(A)** Bright field (*upper panels*) and fluorescent (*second panels*) photos taken from ONL side are shown. Bottom panels in A show immunostained frozen sections with anti-GFP antibody. **(B, C)** Coimmunostaining using antibodies anti-GFP and -TFAP2A for amacrine cell, -CHX10 for bipolar cell, -cyclinD3 for Müller glia, or -photoreceptor-specific nuclear receptor for rod photoreceptors was performed. The numbers of subtype specific protein positive cells in 100 μm vision are shown in **(B)**. Nuclei were visualized by DAPI staining in **(C)**. Values are average of at least three independent samples with standard deviation. *$p < 0.05$ (Student *t*-test). Scale bar in black = 500 μm and white = 50 μm **(A)**. GCL, ganglion cell layer; INL, inner nuclear layer; ONL, outer nuclear layer.

antibodies, which mark apoptotic and proliferative cells, respectively. We found that the downregulation of *Setd1a* led to an increase in apoptotic cells (Fig. 2B) and a dramatic decrease in proliferating cells (Fig. 2C). The decreased EdU incorporation confirmed the decrease in proliferation by the expression of shSetd1a (Fig. 2D). We also found that the thickness of the neuroblast layer, but not that of the ganglion cell layer, decreased in shSetd1a-expressing retinas (Fig. 2E, Supplementary Fig. S1A).

We then examined whether the downregulation of *Setd1a* exerted similar effects on RPCs at earlier stages. EGFP-expressing and shSetd1a-encoding plasmids were electroporated into isolated retinas on E14, and the retinas were cultured for 3 days as explants. The expression of shSetd1a did not affect retinal thickness (Fig. 2F, Supplementary Fig. S1B). In addition, *Setd1a* depletion did not affect the abundance of apoptotic and proliferating cells (Fig. 2G, Supplementary Fig. S1C). The examination of retinal ganglion cells and amacrine cells in early stage retinas revealed that cell numbers did not differ between control and shSetd1a-expressing retinas (Fig. 2G, Supplementary Fig. S1C). When the retinas were cultured for 7 days, we observed thinner neuroblast layer and ganglion cell layer in shSetd1a-expressing retina (Fig. 2I, Supplementary Fig. S1D). Accordingly, an increase in apoptotic cells and a decrease in proliferating cells were observed (Figs. 2H, J), implying that *Setd1a* depletion affects the survival and proliferation of late RPCs. Furthermore, in early-stage retinas, the number of retinal ganglion cells labeled by BRN3B and amacrine cells labeled by HuC/D decreased (Figs. 2H, J).

Effects of shSetd1a on the Differentiation of Late-stage Retinal Cells

The effects of shSetd1a on retinal differentiation were examined. Mouse retinas at E17 were transfected with control or shSetd1a plasmids with EGFP-expressing plasmids and cultured for 14 days as explants. Before they were harvested, the cultured retinas were observed under a bright-field microscope from the ONL side. In shSetd1a-expressing retinas, there were numerous black dots and almost no EGFP-positive cells (Fig. 3A). Examination of frozen sections confirmed that there were only a few

Investigative Ophthalmology & Visual Science

EGFP-positive cells in shSetd1a-expressing retinas, in contrast with control retinas, in which numerous EGFP-positive cells were observed (Fig. 3A, bottom). The results indicated that most of the shSetd1a-expressing cells had probably disappeared via apoptosis during the culture period. We then examined whether there were differences in the abundances of specific retinal cell subtypes. Numbers of TFAP2A-positive amacrine cells were similar between control and shSetd1a-expressing retinas (Figs. 3B, C), whereas there were fewer CHX10-positive bipolar cells, cyclinD3-positive Müller glia, and photoreceptor-specific nuclear receptor-positive rod photoreceptors in shSetd1a-expressing retinas (Figs. 3B, C). The latter three cell subtypes develop during the middle-to-late period of retinal development, implying that *Setd1a* depletion damages late retinal progenitors and decreases the abundance of late-stage retinal cells.

The SET Domain Is Essential for the Prevention of Apoptosis and Induction of Proliferation by Setd1a in Retinal Development

We investigated whether the shSetd1a-induced phenotype was caused by *Setd1a* depletion by performing SETD1A complementation experiments. We first confirmed that ectopic expression of full-length SETD1A (Fig. 4A) in retinal explants did not lead to changes in the numbers of AC3-positive apoptotic cells and Ki67-positive proliferating cells (Figs. 4B–D). Then, shSetd1a and full-length SETD1A were cotransfected into retinas on E17 and cultured for 3 days. SETD1A expression reversed the increase in AC3-positive cell abundance and the decrease in Ki67-positive proliferating cell abundance (Figs. 4B–D).

The SET domain is localized at the SETD1A C-terminus (Fig. 4A) and is responsible for catalyzing H3K4me3.[16] To determine whether the prevention of apoptosis and promotion of proliferation in RPCs by *Setd1a* were mediated by SETD1A catalytic activity, rescue experiments in which shSetd1a-expressing retinas were treated with mutant SETD1A that lacked the SET domain (SETD1AΔSET; Fig. 4A) were performed. Cotransfection of SETD1AΔSET with shSetd1a did not rescue apoptosis and proliferation failure (Figs. 4B–D), indicating that *Setd1a* exerts effects on retinas as observed in earlier experiments through its methyltransferase activity.

Identification of Setd1a Target Gene(s) During Retinal Development Using RNA-Seq

RNA-Seq was performed to investigate the molecular pathways downstream of *Setd1a* activity in the retina. Plasmids encoding shSetd1a or control with an EGFP expression vector were electroporated into E17 retina, and the retinas were cultured for 2 days. EGFP-positive cells were collected via cell sorting and subjected to RNA-Seq (GSE154498) analysis. The gross pattern of changes in gene expression was visualized using a volcano plot (Supplementary Fig. S2A), and there were similar numbers of negatively and positively regulated genes. Genes that were significantly downregulated and upregulated by shSetd1a were selected for further analyses (Supplementary Fig. S2B, Supplementary Table). Initially, we searched for protein-coding genes with a transcripts-per-million value of more than 10. Of these, we selected the genes that were downregulated or upregulated by more than 50% compared with the control (Supplementary Fig. S2B). Gene ontology analysis of the 62 genes showed that the top three categories were related to cell proliferation (Supplementary Fig. S2B). Conversely, according to DAVID ontology analysis, the upregulated genes were assigned to different terms (Supplementary Fig. S2B). The H3K4me3 levels of the downregulated 62 gene loci were examined by using publicly ChIP-Seq data of H3K4me3 in the P1 mouse retina (GSE87064).[32] Of those genes, protein-coding genes and genes associated with H3K4me3 enrichment around the promoter region were selected. Then, genes localized on the XY chromosomes were excluded, and only genes with a peak q score [−10*log(q-value)] of more than 400 were retained. Among the remaining 4976 genes, 17 genes overlapped with the 62 genes identified via RNA-Seq (GSE154498) (Supplementary Fig. S2C, D). Most of the genes detected were associated with cell proliferation, consistent with the results of DAVID ontology analysis. Among those genes, we chose *Uhrf1* as a candidate target gene of *Setd1a*, because UHRF1 was reported to form a complex with SETD1A and maintain bivalent histone marks at cell specification-associated domains in embryonic stem cells.[38]

H3K4me3 Level at the Uhrf1 Locus Is Modulated by the Setd1a Expression Level

The expression pattern of *Uhrf1* transcripts (Fig. 5A) during retinal development was analyzed based on RNA-Seq data on developing mouse retinas (GSE87064). Expression levels of *Uhrf1* transcripts were highest in E14.5 embryonic retinas, then decreased continuously through the rest of retinal development (Fig. 5B). Our RNA-Seq analysis (GSE154498) of shSetd1a showed that the expression levels of *Uhrf1* variants 204 and 207 (Fig. 5A) were significantly lower in shSetd1a-expressing retinas than in control retinas. The expression level of variant 203 also decreased, but the difference was not statistically significant (Fig. 5C). The other two forms, which use the first exon as the start site, were expressed very weakly, and no significant differences were observed between shSetd1a-expressing and control retinas (Fig. 5C). According to publicly available online data (viz.stjude.cloud[32]), two H3K4me3 peaks are associated with the *Uhrf1* locus, around the transcriptional start sites of the first and second exons (Fig. 5D). The association between H3K4me3 and the *Uhrf1* locus was examined via ChIP-qPCR using three primer sets; one for the weakly methylated 5′ region, and two for methylation peaks (Fig. 5D). Plasmids encoding shSetd1a or control with an EGFP expression vector were electroporated into E17 retina, and the retinas were cultured for 2 days. EGFP-positive cells were sorted using a cell sorter and subjected to ChIP-qPCR. Signal levels from reactions using primer C, which amplifies the region around the H3K4me3 peak at the 3′ side, were significantly lower in shSetd1a-expressing retina (Fig. 5E), which is consistent with the lower transcript levels of *Uhrf1* variants 204 and 207 in shSetd1a-expressing retinas (Fig. 5C).

Uhrf1 Knockdown Resulted in Increased Apoptosis and Proliferation Failure in RPCs

We next examined the effects of *Uhrf1* knockdown on retinal development. The *Uhrf1* expression was significantly decreased in the explant retina expressing shUhrf1

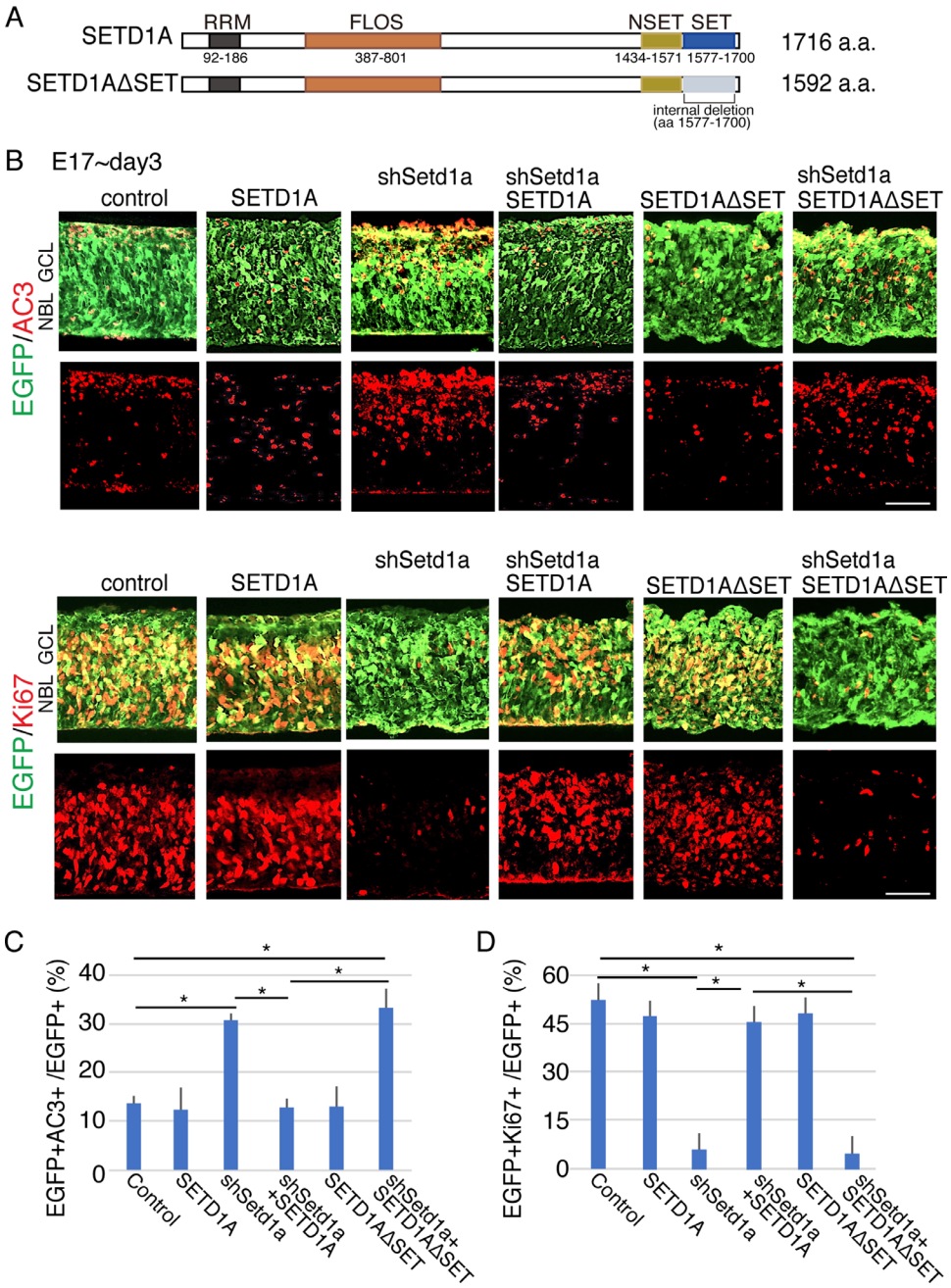

Figure 4. SET domain is essential for the function of Setd1a in retinal development. **(A)**. Schematic representation of SETD1A and SETD1AΔSET (SET domain deleted SETD1A). RRM, RNA recognition motif domain; FLOS, Functional Location on SETD1A; NSET, a region near SET; SET, SET, Su(var)-3-9, Enhancer-of-zeste, Trithorax. **(B–D)** Plasmids encoding control, SETD1A, shSetd1a, SETD1A or SETD1AΔSET and EGFP expression plasmids were transfected as indicated into the retinas from embryos at E17, and cultured for 3 days. Immunostaining was done by using anti-AC3 or -Ki67 with-GFP antibodies **(B)**. The percentages of AC3 and EGFP **(C)**, Ki67 and EGFP **(D)** double-positive cells in total EGFP-positive cells are shown. Values are average of at least three independent samples with standard deviation. *$p < 0.05$ (Tukey's HSD test). Scale bar = 50 µm. GCL, ganglion cell layer; NBL, neuroblastic layer.

(Fig. 6A). We transfected shUhrf1-encoding plasmids with an EGFP expression vector into isolated mouse retinas on E14 and harvested the retinas after 3 days of explant culture. Numbers of AC3-positive cells were almost the same between control and shUhrf1-expressing retinas (Fig. 6B), and the abundance of Ki67-positive proliferating cells also did not differ between control and shUhrf1-expressing retinal cells (Fig. 6C). We then transfected shUhrf1 and EGFP cDNA into retinas on E17 and cultured the retinas for 3 days. The abundance of AC3-positive apoptotic cells increased dramatically (Fig. 6D), and Ki67-positive proliferating cells nearly disappeared (Fig. 6E). The decreased EdU incorporation in the retina expressing shUhrf1 also indicates that the proliferation was severely perturbed by the shUhrf1 expression (Fig. 6F).

To examine the effects of *Uhrf1* loss of function on retinal cell differentiation, we extended the culture period for retinal explants to 14 days. TFAP2A-positive amacrine cells were not affected, but the numbers of CHX10-positive bipolar cells, cyclinD3-positive Müller glia,

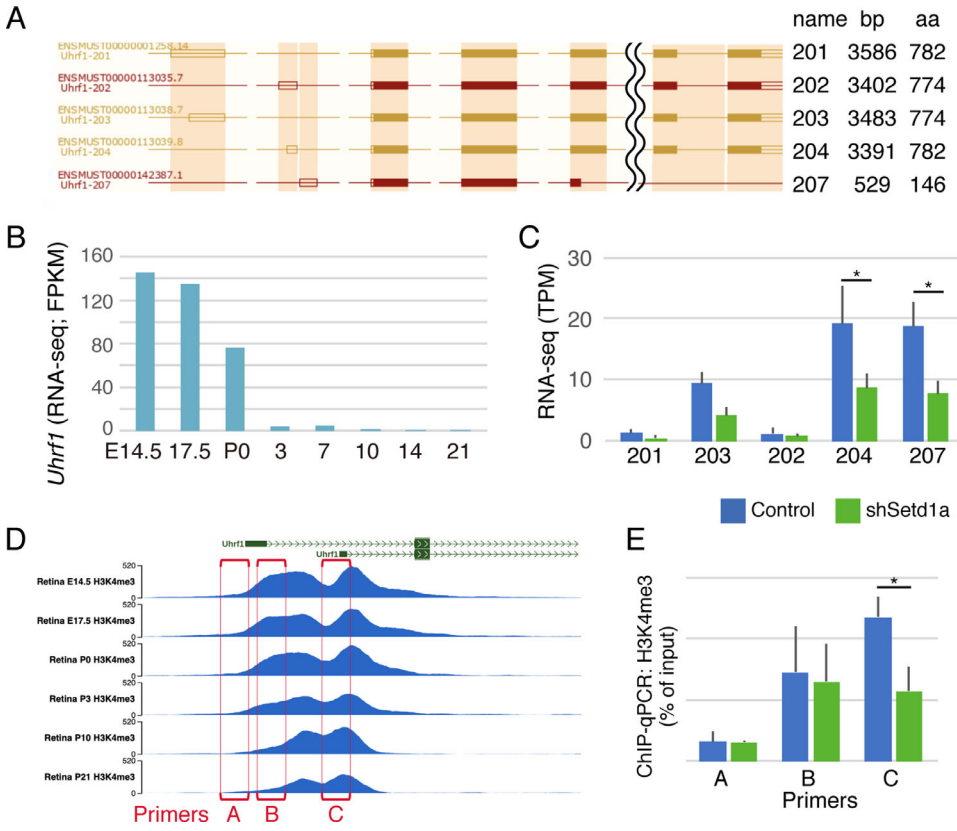

Figure 5. Expression of Uhrf1 transcripts was decreased by the expression of shSetd1. **(A)** Schematic representation of alternative splicing products of *Uhrf1*. Adapted from the schematic data of asia.ensembl.org. **(B)**. Transition of expression level of transcripts of *Uhrf1* during mouse retinal development from RNA-Seq data of whole mouse retina (GSE87064).[32] **(C)** Retinas at E17 were transfected with control or shSetd1a plasmids with an EGFP expression vector and cultured 2 days. EGFP positive-cells were purified, and RNA-Seq was performed. Expression levels of *Uhrf1* splicing variants in the control or shSet1a-expressing retinas are shown. Values are average of 3 or 4 samples of RNA-Seq (GSE154498) data with standard deviation. *q < 0.05 (false discovery rate). TPM, transcripts per million. **(D)** H3K4me3 levels at *Uhrf1* locus during mouse retinal development from ChIP-Seq data of whole mouse retina (viz.stjude.cloud). Locus of three primer sets for ChIP-qPCR **(E)** are shown in the *red box*. **(E)** The retinas at E17 were transfected with control or shSetd1a with EGFP expression plasmids and cultured for 2 days. EGFP-positive cells were collected and subjected to ChIP-qPCR using anti-H3K4me3 antibody. *Uhrf1* promoter regions were amplified by using three different primer sets. Values are average of at least three independent samples with standard deviation. *p < 0.05 (Student t-test).

and photoreceptor-specific nuclear receptor-positive rod photoreceptors decreased in shUhrf1-expressing retinas (Supplementary Fig. S3A, B).

Upon cotransfection of full-length UHRF1 and shUhrf1 expression plasmids, the increase in apoptotic cells and decrease in proliferating cells induced by *Uhrf1* depletion were reversed (Fig. 6D, E). The expression of full-length UHRF1 alone did not affect apoptosis and proliferation in the retina (Fig. 6D, E). Finally, to determine whether the ectopic expression of UHRF1 reverses the shSetd1a-induced phenotype, UHRF1 was coexpressed with shSetd1a. Coexpression led to an increase in apoptotic cells, but UHRF1 expression reversed the shSetd1a-induced inhibition of proliferation (Fig. 6D, E), implying that apoptosis and proliferation are regulated by different mechanisms.

Uhrf1 Depletion Did Not Lead to Changes in Bulk DNA Methylation in the Retina

Uhrf1 is a hemimethylated DNA-binding protein and facilitates DNA methylation by recruiting *Dnmt1*.[39–41] We investigated whether loss of *Uhrf1* contributes to global DNA hypomethylation in the retina by immunostaining to detect 5mC. Plasmids encoding shUhrf1 with an EGFP-expressing vector were transfected into isolated retinas on E17, and the retinas were harvested after 3 days. Because apoptotic cells can create noise in the background with 5mC staining,[42] shUhrf1-expressing retinas were cultured with ZVAD, an apoptosis inhibitor.[43] No AC3-positive apoptotic cells were observed after treatment with ZVAD (Supplementary Fig. S4A). Then, retinal sections were stained with the anti-5mC antibody. The 5mC signal intensities did not differ between ZVAD-treated control and shUhrf1-expressing cells (Supplementary Fig. S4B). For the control, retinas were treated with 1 µM 5-Aza (A3656; Sigma-Aldrich, St. Louis, MO), an inhibitor of DNMT1 that lead to DNA hypomethylation. After 3 days, the retinas were frozen and sectioned. At 1 µM of 5-Aza, proliferation was only slightly suppressed, and the number of apoptotic cells increased slightly (Supplementary Fig. S4C). Additionally, 5mC signal intensities seemed to decrease in the presence of 5-Aza (Supplementary Fig. S4C), indicating that the antibody could detect methylated DNA.

Investigative Ophthalmology & Visual Science

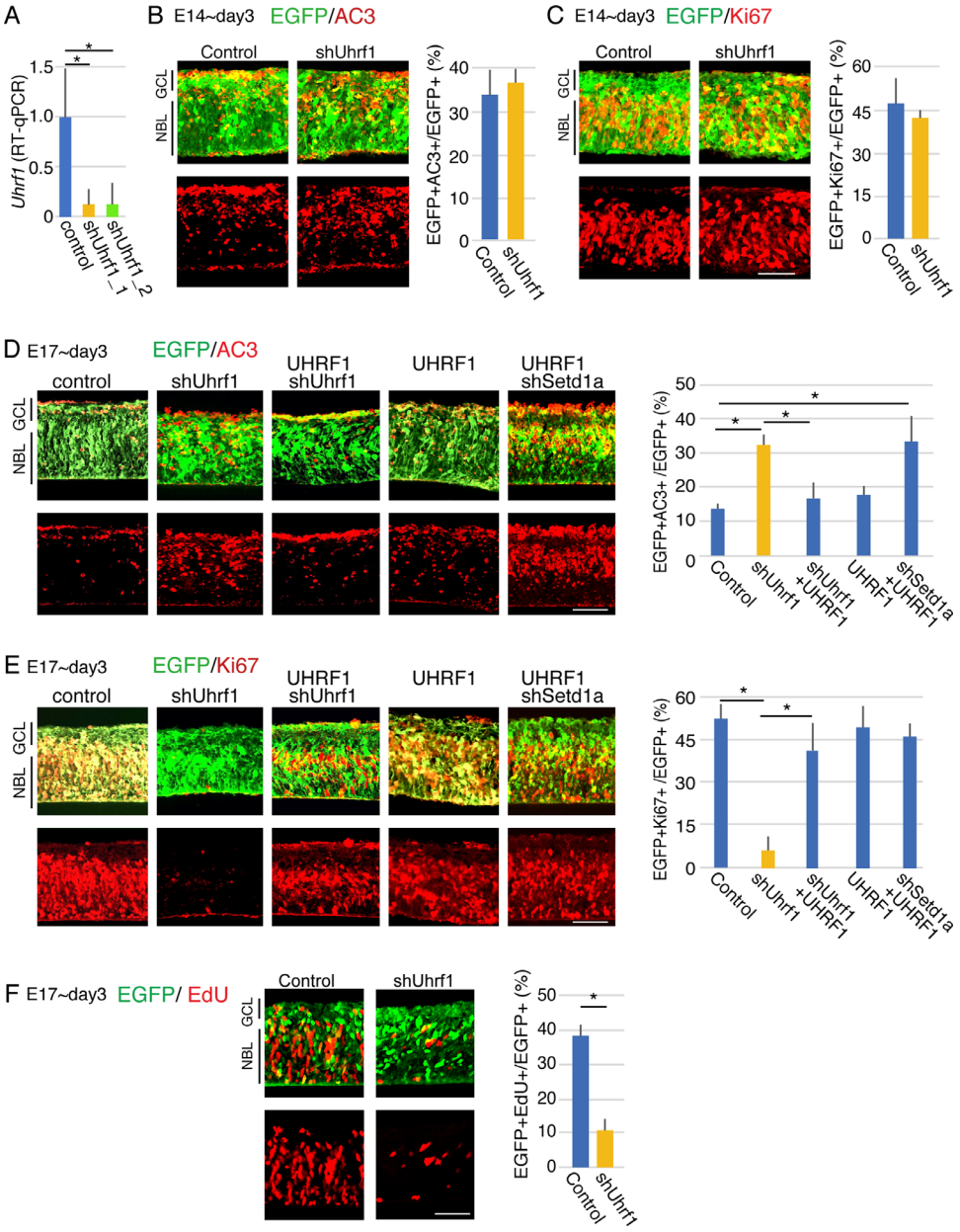

Figure 6. Expression of shUhrf1 perturbed retinal development. Plasmids encoding control, shUhrf1, UHRF1, or shSetd1a and EGFP expression plasmids were electroporated into mouse retina at E14 **(B, C)** or E17 **(A, D–F)**. Combination of transfected plasmids are indicated in the figures. **(A)** After sorting EGFP-positive cells, total RNA was purified and served to RT-qPCR. The averages of three independent samples with standard deviations are shown. *$p < 0.05$ (Student *t*-test). **(B–E)** Immunostaining using anti-AC3 **(B, D)** or anti-Ki67 **(C, E)** with -EGFP antibodies was done. **(F)** The incorporated EdU was detected by a click reaction. The percentages of EGFP and AC3 **(B, D)**, EGFP and Ki67 **(C, E)**, or EGFP and EdU **(F)** double-positive cells in the total EGFP-positive cells are shown. Values are average of three independent samples with standard deviation. *$p < 0.05$ (Student *t*-test or Tukey's HSD test). Scale bar = 50 µm. GCL, ganglion cell layer; NBL, neuroblastic layer.

Discussion

At least nine methyltransferases and five demethylases have been reported to target histone H3K4me1/2/3 as a substrate in mammals.[13,15] H3K4 methylation is reported to be involved in rod photoreceptor development during retinal development.[6,11,44] Here, we investigated the roles H3K4 methylation plays in RPCs and the expression patterns of related genes using previously published RNA-Seq data.[32] We found that *Kmt2c* and *Kmt2b* are expressed from the early stages of retinal development, whereas other genes were expressed at low levels and *Setd1b*/*Kmt2g* at very low levels (Supplementary Fig. S5). As a preliminary study, we performed a miniscreening of the functions of H3K4 methylases and demethylases during early retinal development using an shRNA-mediated loss-of-function approach with retinal explant culture. We found that several shRNAs disrupted retinal development; among them, shSetd1a exerted the strongest effects, by inducing apoptosis and suppressing proliferation. Therefore, we focused on analyzing the functions of *Setd1a* during early retinal development.

Among methyltransferases, *Setd1a* exerts strong effects and performs a unique function; thus, other methylases could not compensate for the loss in function when *Setd1a* was depleted. Methylases can be divided into several subgroups according to their structure.[9] *Setd1a* and *Setd1b* belong to a subgroup characterized by the presence of an RRM domain[45] in addition to the FLOS region.[19] The C-terminal SET domain is found in all H3K4 methyltransferases; hence, it is possible that the RRM and/or FLOS domains contribute to SETD1A function. Although SETD1B has the same domains as SETD1A, it is unlikely that it can replace SETD1A because it is expressed at low levels (Supplementary Fig. S5). In fact, although we transfected shSetd1b in addition to shSetd1a into the E14 retina, we did not observe perturbation of proliferation nor cell death of early retinal progenitors (Supplementary Fig. S6).

Uhrf1 was identified as a possible downstream gene target of *Setd1a*. Because UHRF1 overexpression rescued the shSetd1a-induced suppression of proliferation, SETD1A may induce cell proliferation by inducing UHRF1. By contrast, UHRF1 expression did not reverse the induction of apoptosis in the absence of SETD1A, indicating that either the inhibition of apoptosis by SETD1A does not depend on UHRF1 or that both SETD1A and UHRF1 are necessary for the process, which is more likely because SETD1A and UHRF1 form a complex.[38] UHRF1 binds to hemi-methylated DNA to recruit DNMT1, leading to DNA methylation.[46–48] *Dnmt1* and *Dnmt3a/b* are reported to be involved in photoreceptor and outer plexiform layer development during mammalian retinal development,[48] and *Dnmt1*-dependent DNA methylation is essential for photoreceptor-terminal differentiation and retinal neuron survival.[49] We did not observe marked changes in DNA methylation in the absence of *Uhrf1*, but differences in retinal phenotypes induced by *Dnmt1* and *Uhrf1* depletion indicate that the outcomes of shUhrf1 expression in the retina cannot be explained by the disruption of DNA methylation alone. *Uhrf1* is reported to be involved in regulating H3K4me3 in collaboration with *Setd1a* in embryonic stem cells.[38] UHRF1 forms a complex with SETD1A/COMPASS and regulates neuroectoderm and mesoderm differentiation.[38] We did not directly analyze the regulation of differentiation of retinal cell subtypes by SETD1A or UHRF1, but the involvement of such collaborative mechanisms in the prevention of apoptosis is feasible.

Interestingly, DAVID ontology analysis of the differentially expressed genes in shSetd1a-expressing retinas (as detected using RNA-Seq) showed that the genes were mostly associated with cell proliferation. We hypothesize that *Setd1a* enhances the transcriptional activation of these proliferation-related genes through its H3K4 methyltransferase activity. In contrast, *Setd1a*-induced methylation and transcriptional activation may be regulated independently, as reported in yeast and flies. In *Saccharomyces cerevisiae*, SET1 methylates DAM1, a protein involved in kinetochore assembly and chromosome segregation,[50] and in *S pombe*, SET1 participates in the silencing and genome organization of retrotransposons independently of H3K4 methylation activity.[51] In *Drosophila*, H3K4A mutations abolish global H3K4 methylation but not transcriptional activity.[52] In mammals, deletion of the SET1 complex subunit CFP1 in mouse embryonic stem cells results in a global decrease of H3K4me3 in CpG island promoters. However, transcription levels did not change.[53] Although the suppression of proliferation-related genes including *Uhrf1* is a major reason explaining the loss of proliferation activity in RPCs, transcription-independent mechanisms should also be considered.

The specific deletion of *Setd1a* in adult long-term hematopoietic stem cells resulted in the loss of proliferative capacity and a failure to repair DNA damage in these cells.[54] However, according to our RNA-Seq analysis, shSetd1a did not affect expression of the genes selected for analysis. Abnormalities in the H3K4 methyltransferases MLL1, MLL3, and MLL4 have been shown to result in cancer and hematopoietic malignancies.[55] In addition, in MLL-AF9 leukemia, SETD1A is required for cell survival and leukemia progression in vitro as well as in vivo.[19] It should be noted that we performed this study in retinal explants, which has limitation to reproduce all the biological phenomena occur in in vivo because additional stress to the retina by making the explant culture may affect the results. However, we believe that the explant culture system is an excellent tool to get essential information of the effects of gene manipulation quick and easily, and further analysis by using mouse model may extend current findings. Taken together, these findings indicate that *Setd1a* is strongly associated with cell proliferation and survival, but some tissue-specific mechanisms that regulate *Setd1a* function remain to be determined.

Acknowledgments

The authors thank Shizuka Ohmura for her contribution of initial plan of this project, and Asano Tsuhako and Miho Nagoya for technical supports.

Supported by JSPS KAKENHI (16H06279 for S. Watanabe, 15H04695 for S. Watanabe, 18K16949 for T. Iwagawa).

Disclosure: **X. Deng,** None; **T. Iwagawa,** None; **M. Fukushima,** None; **Y. Suzuki,** None; **S. Watanabe,** None

References

1. Margueron R, Reinberg D. The Polycomb complex PRC2 and its mark in life. *Nature*. 2011;469(7330):343–349.
2. Swaroop A, Kim D, Forrest D. Transcriptional regulation of photoreceptor development and homeostasis in the mammalian retina. *Nat Rev Neurosci*. 2010;11(8):563–576.
3. Cepko C. Intrinsically different retinal progenitor cells produce specific types of progeny. *Nat Rev Neurosci*. 2014;15(9):615–627.
4. Corso-Díaz X, Jaeger C, Chaitankar V, Swaroop A. Epigenetic control of gene regulation during development and disease: a view from the retina. *Prog Retin Eye Res*. 2018;65:1–27.
5. Zelinger L, Swaroop A. RNA biology in retinal development and disease. *Trends Genet*. 2018;34(5):341–351.
6. Iwagawa T, Watanabe S. Molecular mechanisms of H3K27me3 and H3K4me3 in retinal development. *Neurosci Res*. 2018;138:43–48.
7. Iida A, Iwagawa T, Baba Y, et al. Roles of histone H3K27 trimethylase Ezh2 in retinal proliferation and differentiation. *Dev Neurobiol*. 2015;75(9):947–960.
8. Umutoni D, Iwagawa T, Baba Y, et al. H3K27me3 demethylase UTX regulates the differentiation of a subset of bipolar cells in the mouse retina. *Genes Cells*. 2020;25(6):402–412.
9. Shen E, Shulha H, Weng Z, Akbarian S. Regulation of histone H3K4 methylation in brain development and disease. *Philos Trans R Soc Lond B Biol Sci*. 2014;369:1652.
10. Hao H, Kim DS, Klocke B, et al. Transcriptional regulation of rod photoreceptor homeostasis revealed by in vivo NRL targetome analysis. *PLoS Genet*. 2012;8(4):e1002649.

11. Ueno K, Iwagawa T, Kuribayashi H, et al. Transition of differential histone H3 methylation in photoreceptors and other retinal cells during retinal differentiation. *Sci Rep*. 2016;6:29264.
12. Shilatifard A. The COMPASS family of histone H3K4 methylases: mechanisms of regulation in development and disease pathogenesis. *Annu Rev Biochem*. 2012;81:65–95.
13. Davie JR, Xu W, Delcuve GP. Histone H3K4 trimethylation: dynamic interplay with pre-mRNA splicing1. *Biochem Cell Biol*. 2015;94(1):1–11.
14. Qu Q, Takahashi YH, Yang Y, et al. Structure and conformational dynamics of a COMPASS histone H3K4 methyltransferase complex. *Cell*. 2018;174(5):1117–1126.e12.
15. Crump NT, Milne TA. Why are so many MLL lysine methyltransferases required for normal mammalian development? *Cell Mol Life Sci*. 2019;76(15):2885–2898.
16. Bledau AS, Schmidt K, Neumann K, et al. The H3K4 methyltransferase Setd1a is first required at the epiblast stage, whereas Setd1b becomes essential after gastrulation. *Development (Cambridge)*. 2014;141(5):1022–1035.
17. Higgs MR, Sato K, Reynolds JJ, et al. Histone methylation by SETD1A protects nascent DNA through the nucleosome chaperone activity of FANCD2. *Mol Cell*. 2018;71(1):25–41.e6.
18. Tajima K, Matsuda S, Yae T, et al. SETD1A protects from senescence through regulation of the mitotic gene expression program. *Nature Commun*. 2019;10(1):1–13.
19. Hoshii T, Cifani P, Feng Z, et al. A non-catalytic function of SETD1A regulates cyclin K and the DNA damage response. *Cell*. 2018;172(5):1007–1021.e17.
20. Mukai J, Cannavò E, Crabtree GW, et al. Recapitulation and reversal of schizophrenia-related phenotypes in Setd1a-deficient mice. *Neuron*. 2019;104(3):471–487.e12.
21. Takata A, Xu B, Ionita-Laza I, Roos JL, Gogos JA, Karayiorgou M. Loss-of-function variants in schizophrenia risk and SETD1A as a candidate susceptibility gene. *Neuron*. 2014;82(4):773–780.
22. Singh T, Kurki MI, Curtis D, et al. Rare loss-of-function variants in SETD1A are associated with schizophrenia and developmental disorders. *Nature Neurosci*. 2016;19(4):571–577.
23. Satoh S, Tang K, Iida A, et al. The spatial patterning of mouse cone opsin expression is regulated by bone morphogenetic protein signaling through downstream effector COUP-TF nuclear receptors. *J Neurosci*. 2009;29(40):12401–12411.
24. Tabata Y, Ouchi Y, Kamiya H, Manabe T, Arai K, Watanabe S. Specification of the retinal fate of mouse embryonic stem cells by ectopic expression of Rx/rax, a homeobox gene. *Mol Cell Biol*. 2004;24(10):4513–4521.
25. Iida A, Shinoe T, Baba Y, et al. Dicer plays essential roles for retinal development by regulation of survival and differentiation. *Invest Ophthalmol Vis Sci*. 2004;52(10):4513–4521.
26. Shinoe T, Kuribayashi H, Saya H, Seiki M, Aburatani H, Watanabe S. Identification of CD44 as a cell surface marker for Müller glia precursor cells. *J Neurochem*. 2010;115(6):1633–1642.
27. Patro R, Duggal G, Love MI, Irizarry RA, Kingsford C. Salmon provides fast and bias-aware quantification of transcript expression. *Nat Methods*. 2017;14(4):417–419.
28. Bray NL, Pimentel H, Melsted P, Pachter L. Near-optimal probabilistic RNA-seq quantification. *Nat Biotechnol*. 2016;34(5):525–527.
29. Huang DW, Sherman BT, Lempicki RA. Systematic and integrative analysis of large gene lists using DAVID bioinformatics resources. *Nat Protoc*. 2009;4(1):44–57.
30. Huang DW, Sherman BT, Lempicki RA. Bioinformatics enrichment tools: paths toward the comprehensive functional analysis of large gene lists. *Nucleic Acids Res*. 2009;37(1):1–13.
31. Iida A, Iwagawa T, Kuribayashi H, et al. Histone demethylase Jmjd3 is required for the development of subsets of retinal bipolar cells. *Proc Natl Acad Sci USA*. 2014;111(10):3751–3756.
32. Aldiri I, Xu B, Wang L, et al. The dynamic epigenetic landscape of the retina during development, reprogramming, and tumorigenesis. *Neuron*. 2017;94(3):550–568.e10.
33. Langmead B, Salzberg SL. Fast gapped-read alignment with Bowtie 2. *Nat Methods*. 2012;9(4):357–359.
34. Li H, Handsaker B, Wysoker A, et al. The sequence alignment/map format and SAMtools. *Bioinformatics*. 2009;25(16):2078–2079.
35. Li H. A statistical framework for SNP calling, mutation discovery, association mapping and population genetical parameter estimation from sequencing data. *Bioinformatics*. 2011;27(21):2987–2993.
36. Zhang Y, Liu T, Meyer CA, et al. Model-based analysis of ChIP-Seq (MACS). *Genome Biol*. 2008;9(9):R137.
37. Yu G, Wang LG, He QY. ChIP seeker: an R/Bioconductor package for ChIP peak annotation, comparison and visualization. *Bioinformatics*. 2015;31(14):2382–2383.
38. Kim KY, Tanaka Y, Su J, et al. Uhrf1 regulates active transcriptional marks at bivalent domains in pluripotent stem cells through Setd1a. *Nat Commun*. 2018;9(1):2583.
39. Rothbart SB, Krajewski K, Nady N, et al. Association of UHRF1 with methylated H3K9 directs the maintenance of DNA methylation. *Nat Struct Mol Biol*. 2012;19(11):1155–1160.
40. Rothbart SB, Dickson BM, Ong MS, et al. Multivalent histone engagement by the linked tandem tudor and PHD domains of UHRF1 is required for the epigenetic inheritance of DNA methylation. *Genes Dev*. 2013;27(11):1288–1298.
41. Hahm JY, Park JW, Kang JY, et al. Acetylation of UHRF1 regulates hemi-methylated DNA binding and maintenance of genome-wide DNA methylation. *Cell Rep*. 2020;32(4):107958.
42. Wahlin KJ, Enke RA, Fuller JA, Kalesnykas G, Zack DJ, Merbs SL. Epigenetics and cell death: DNA hypermethylation in programmed retinal cell death. *PLoS One*. 2013;8(11):e79140.
43. Swe M, Sit KH. zVAD-fmk and DEVD-cho induced late mitosis arrest and apoptotic expressions. *Apoptosis*. 2000;5(1):29–36.
44. Kizilyaprak C, Spehner D, Devys D, Schultz P. In Vivo chromatin organization of mouse rod photoreceptors correlates with histone modifications. *PLoS One*. 2010;5(6):e11039.
45. Lee JH, Skalnik DG. Rbm15-Mkl1 interacts with the Setd1b histone H3-Lys4 methyltransferase via a SPOC domain that is required for cytokine-independent proliferation. *PLoS One*. 2012;7(8):e42965.
46. Bostick M, Jong KK, Estève PO, Clark A, Pradhan S, Jacobsen SE. UHRF1 plays a role in maintaining DNA methylation in mammalian cells. *Science*. 2007;317(5845):1760–1764.
47. Bronner C, Fuhrmann G, Chédin FL, Macaluso M, Dhe-Paganon S. UHRF1 links the histone code and DNA methylation to ensure faithful epigenetic memory inheritance. *Genet Epigenet*. 2009;2009(2):29–36.
48. Singh RK, Mallela RK, Hayes A, et al. Dnmt1, Dnmt3a and Dnmt3b cooperate in photoreceptor and outer plexiform layer development in the mammalian retina. *Exp Eye Res*. 2017;159:132–146.
49. Rhee KD, Yu J, Zhao CY, Fan G, Yang XJ. Dnmt1-dependent DNA methylation is essential for photoreceptor terminal differentiation and retinal neuron survival. *Cell Death Dis*. 2012;3(11):e427.

Investigative Ophthalmology & Visual Science

50. Zhang K, Lin W, Latham JA, et al. The Set1 methyltransferase opposes Ipl1 Aurora kinase functions in chromosome segregation. *Cell*. 2005;122(5):723–734.
51. Lorenz DR, Mikheyeva I V., Johansen P, et al. CENP-B cooperates with set1 in bidirectional transcriptional silencing and genome organization of retrotransposons. *Mol Cell Biol*. 2012;32(20):4215–4225.
52. Hödl M, Basler K. Transcription in the absence of histone H3.2 and H3K4 methylation. *Curr Biol*. 2012;22(23):2253–2257.
53. Clouaire T, Webb S, Skene P, et al. Cfp1 integrates both CpG content and gene activity for accurate H3K4me3 deposition in embryonic stem cells. *Genes Dev*. 2012;26(15):1714–1728.
54. Arndt K, Kranz A, Fohgrub J, et al. SETD1A protects HSCs from activation-induced functional decline in vivo. *Blood*. 2018;131(12):1311–1324.
55. Kranz A, Anastassiadis K. The role of SETD1A and SETD1B in development and disease. *Biochim Biophys Acta Gene Regul Mech*. 2020;1863(8):194578.

Investigative Ophthalmology & Visual Science